Journal of Organometallic Chemistry 957 (2022) 122144

Contents lists available at ScienceDirect

Journal of Organometallic Chemistry

journal homepage: www.elsevier.com/locate/jorganchem

Computational investigation of the effect of alkoxy carbon substitution on the mechanism of carbonyl group reduction by 1-hydridosilatranes

Alexander S. Pixler, Ashley M. DeLio[1], Sami E. Varjosaari[2], Vladislav Skrypai, Marc J. Adler[3], Thomas M. Gilbert*

Department of Chemistry and Biochemistry, Northern Illinois University, DeKalb, IL 60115 USA

ARTICLE INFO

Article history:
Received 13 August 2021
Revised 14 October 2021
Accepted 21 October 2021
Available online 24 October 2021

Keywords:
Silatrane
Hydridosilatrane
Carbonyl reduction, Cage
Mechanism

ABSTRACT

We undertook computational investigations to determine the effects of the electronic nature of the cage atoms on the energetics of the reduction of acetone by 1-hydridosilatranes. QTAIM analyses of the parent 1-hydridosilatrane **1H$_6$** and hexasubstituted silatranes **1Me$_6$** and **1F$_6$** showed that the change in charge induced by the donor/acceptor properties of the substituents remained almost entirely localized on the alkoxy carbon; the hydridic nature of the silicon-bound hydrogen as gauged by the charge remained essentially unchanged. This shows resilience to the electronic effects of the substituents at this position. The energetics of acetone reduction to 2-propanol were mapped out for all three cases. Calculations showed favorable Gibbs free energies for each reduction, with considerable exergonicities and modest barriers. Reductions using **1H$_6$** and **1Me$_6$** follow hydride transfer mechanisms without involvement of carbonyl oxygen that lead to an ion/neutral pair, while reduction using **1F$_6$** seems to involve a concerted σ-metathesis-like mechanism that leads directly to a dialkoxysilatrane.

© 2021 Elsevier B.V. All rights reserved.

1. Introduction

Fig. 1 shows the cage structure of silatrane molecules and lists the shorthand names of the molecules examined in this work. Dative donation from the nitrogen to the silicon stabilizes the cage structure [1–5]. Other atranes including stannatranes [6], germatranes [4], and titanatranes [7] show similar interactions. The transannular M···N distance seems to correlate with interaction strength, as it decreases when the silicon is made more Lewis acidic through placement of electron-withdrawing substituents X at position 1 (Fig. 1) [3,8].

While the effect of substitution at position 1 is well studied, that resulting from substitution at the alkoxy carbon positions 3, 7, and 10 remains underdeveloped. Relevant to our work here, Voronkov *et al.* showed through IR spectroscopy that addition of methyl groups at these carbons reduced the strength of the silicon-hydrogen bond in hydridosilatranes, as evidenced by a slight decrease in the Si–H stretching vibration energy. [9] Other work showed that 1-alkyl-3,7,10-trimethyl- [10] and 1-phenyl-3,3,7,7,10,10-hexamethylsilatranes [11,12] resisted solvolysis, [13] making the unknown **1Me$_6$** (Fig. 1) an intriguing candidate for study. Similarly, we thought that **1F$_6$** might resist acidolysis similarly to 3,7,10-tris-trifluoromethyl-1-hydridosilatrane, which dissolves unchanged in trifluoroacetic acid (TFA) [14]. This might prove synthetically useful because open chain silanes can reduce ketones in TFA to trifluoroacetate esters [15]. Similar reactivity of 3,7,10-tris-trifluoromethyl-1-hydridosilatrane has not appeared in the literature, but it and **1F$_6$** would likely prove more soluble and stable in TFA and still capable of reducing ketones. Further reactions of trifluoroacetate esters result in trifluoromethylphenyl compounds [16] used as precursors for important pharmaceuticals such as Fluoxetine [17].

We previously reported investigations of the reducing ability of 1-hydridosilatrane, **1H$_6$**, building on initial work from Eaborn and coworkers [18]. When used in combination with an activator, **1H$_6$** chemo- and stereoselectively reduced ketones and aldehydes to alcohols [19–22]. In the presence of primary and secondary amines, it reduced ketones and aldehydes to secondary and tertiary amines (reductive amination) with some stereoselectivity [23,24], and in the presence of carboxylic acids reduced aldehydes to acylated primary alcohols [25]. We theorized that nitrogen donation to silicon increased the hydrogen hydridity and reactivity compared to that

* Corresponding author.
E-mail address: tgilbert@niu.edu (T.M. Gilbert).
[1] Present address: Department of Chemistry, University of Illinois at Urbana-Champaign, Urbana, IL 61801 USA, and National Center for Supercomputing Applications, University of Illinois at Urbana-Champaign, Urbana, IL 61801, USA.
[2] Present address: Department of Chemistry, Coker University, Hartsville, SC 29550, USA.
[3] Present address: Department of Chemistry and Biology, Ryerson University, Toronto, Ontario M5B 2K3 Canada.

https://doi.org/10.1016/j.jorganchem.2021.122144
0022-328X/© 2021 Elsevier B.V. All rights reserved.

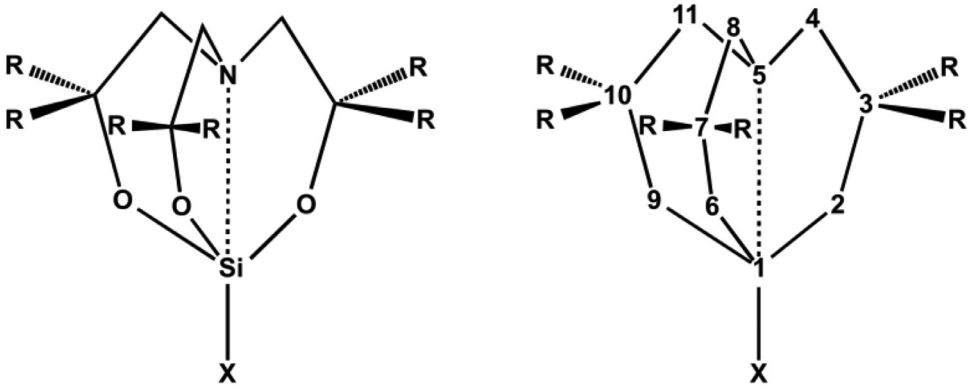

Fig. 1. Generic structure and abbreviations of silatranes investigated, and a diagram showing the conventional position labeling for silatranes.

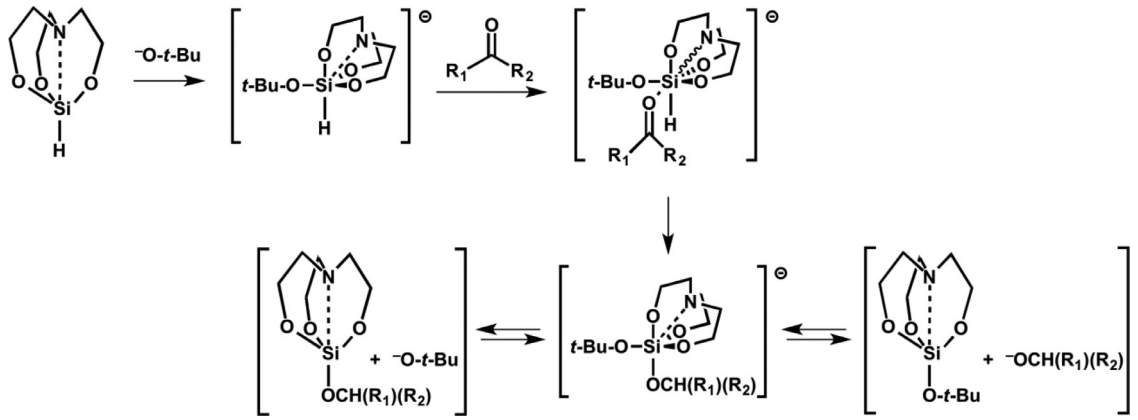

Scheme 1. Mechanism proposed by James [25] for reduction of aldehydes and ketones to alcohols using 1-hydridosilatrane.

in other reducing silanes [26] such as triethoxysilane [27], polymethylhydrosiloxane [28], and other pentacoordinate silicon compounds [29]. Scheme 1 shows a generic reaction mechanism for the reduction of a carbonyl-containing species by **1H$_6$**; we proposed this [21,25] based on earlier work from Corriu [30] and Schiffers et al. [31]. The required *t*-butoxide activator attaches to the five-coordinate 1-hydridosilatrane to form a six-coordinate (*t*-butoxy)hydridosilatrane anion, expanding the coordination sphere of the silicon and increasing hydridic reactivity. Acetone then coordinates to the silicon through the carbonyl oxygen, possibly with concomitant loss of the Si···N interaction to keep the coordination number six, whereupon hydride transfer occurs, forming a dialkoxide. Possibly the dialkoxide hydrolyzes on workup to form the alcoholic product; however, we found evidence for the presence of free alkoxide ions in some reaction solutions. Consequently one anticipates equilibria between the ion/neutral species at the bottom of the scheme, any of which could hydrolyze to the final alcohols.

In this study, we computationally compared the mechanistic components in Scheme 1 and their energetics for the reduction of acetone by the parent 1-hydridosilatrane **1H$_6$** and by 1-hydridosilatranes with the 3, 7, and 10 alkoxy carbons of the silatrane cage fully substituted with electron-donating methyl (**1Me$_6$**) or electron-withdrawing fluorine (**1F$_6$**) substituents. We chose acetone as a computationally efficient proxy for the general reduction of aldehydes and ketones. Examinations of the potential energy surfaces showed favorable energetics for reduction in each case. However, the surface scans indicated that carbonyl oxygen coordination to silicon as shown in Scheme 1 was implausible, and other hydride transfer steps were more likely. When **1H$_6$** or **1Me$_6$** act as reducing agents, hydride transfer occurs directly, without oxygen coordination. When **1F$_6$** is the reductant, direct hydride transfer requires high energy owing to the need to separate the "anionic" hydride from the silicon of the electron-poor hexafluorosilatrane, so a more likely mechanism involves a concerted process that resembles transition metal σ-bond metathesis. The overall favorable energetics for each system indicate that **1Me$_6$** and **1F$_6$** should mimic **1H$_6$** as reductants and may provide alternative reactivity.

2. Computational methods

All calculations were performed using the Gaussian (G09) suite [32]. Reaction components were fully optimized without constraints using the density functional theory (DFT) ωB97XD [33]/6-311+(+)G(d,p) model chemistry. We previously showed that this model chemistry performed particularly well in locating transition states for hydride transfers [34]. The 6-311+(+)G(d,p) designation means the 6-311+G(d,p) basis set was applied to all atoms, and an extra diffuse function was applied to the silicon-bound hydride or the $OCHMe_2$ methylene hydrogen, whichever was appropriate. Including this extra function aided in locating hydride trans-

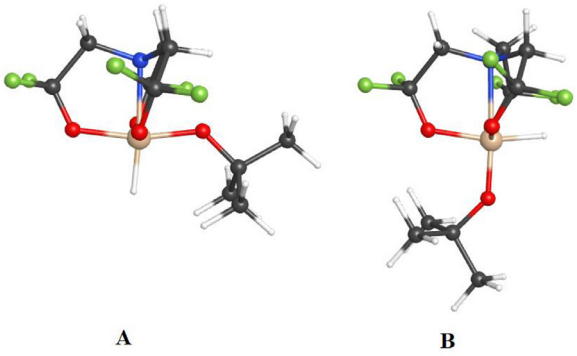

Fig. 2. H*trans* (A) and H*cis* (B) isomers of $2F_6$.

fer transition states [34,35]. This basis set was used throughout, so will not be referred to hereafter. A large integration grid (keyword Int(UltraFineGrid)) was used in all optimizations. Analytical frequency calculations were performed to ensure that optimized minima exhibited only real frequencies while optimized transition states exhibited one imaginary frequency, and to obtain Gibbs free energy corrections. These were used without scaling to correct the raw data to ΔG_{298} values. For cases **2R$_6$** and **6R$_6$**, multiple silatrane conformers were optimized to determine the lowest energy geometries. The examples of the H*trans* and H*cis* isomers of **2F$_6$** appear in Fig. 2; *trans* and *cis* indicate the position of the hydrogen with respect to the cage nitrogen atom. Relative isomer energies appear in Supporting Information Table S3.

Scans of PESes were performed as relaxed scans, meaning that only one parameter was fixed, and all others were unconstrained. As checks on the data, we occasionally used the M062x/6-311+G(d,p) model chemistry for scans rather than the ωB97XD/6-311+(+)G(d,p) model chemistry.

That transition states connected the relevant reactants and products was confirmed by visualizing the imaginary vibrations using the WebMO interface [36]. This was also used for molecular graphics in Figures below. Kaleidagraph for Macintosh [37] was used to generate energy data graphs. We performed charge calculations using the AIMAll program and the ωB97XD wave functions [38]. The program utilized the Quantum Theory of Atoms in Molecules (QTAIM) [39–41].

3. Results and discussion

3.1. Charge distribution analysis

Prior to beginning the mechanistic study, we probed the electronic effects of full substitution at the 3, 7, and 10 alkoxy carbons as well as at the 1 position. Fig. 1 lists the investigated silatranes; Table 1 shows their electronic natures in the form of QTAIM charges. The expected relationship between the charge on Si and the Si···N distance is observed for **1FH$_6$**, which exhibits the most highly positive Si and the shortest Si···N distance. However, this does not hold for the other four silatranes, which exhibit nearly identical Si charges but widely varying Si···N distances. It is particularly notable that although the Si charge is identical for the **1R$_6$** triad, the R = H case exhibits an Si···N distance *ca.* 10 pm longer than does the R = Me case, which in turn is longer than the R = F case by only *ca.* 6 pm. It is difficult to reconcile these relationships with the charges on Si or the alkoxy carbons. The trend does not follow those of other cage size-determining parameters such as the N–C–C–O or C–N–Si–O torsion angles (H > F > Me and F > H > Me, respectively).

The charge data show that charge transfer throughout the cage is essentially nonexistent, regardless of the donor/acceptor nature of the substituents. One sees that the alkoxy carbons on **1F$_6$** are more positively charged than their correspondents in the other cases, but the charges on all other atoms are nearly identical. This holds even for 1-fluorosilatrane **1FSH$_6$** and 1-methylsilatrane **1MeSH$_6$**, which only slightly affect the charge on the silicon to which they are attached, and not the charge on atoms farther away.

The hexamethylhydridosilatrane **1Me$_6$** and the hexafluorohydridosilatrane **1F$_6$** exhibit charges indicating hydridic nature similar to that of the parent **1H$_6$**, providing hope that they might act as re-

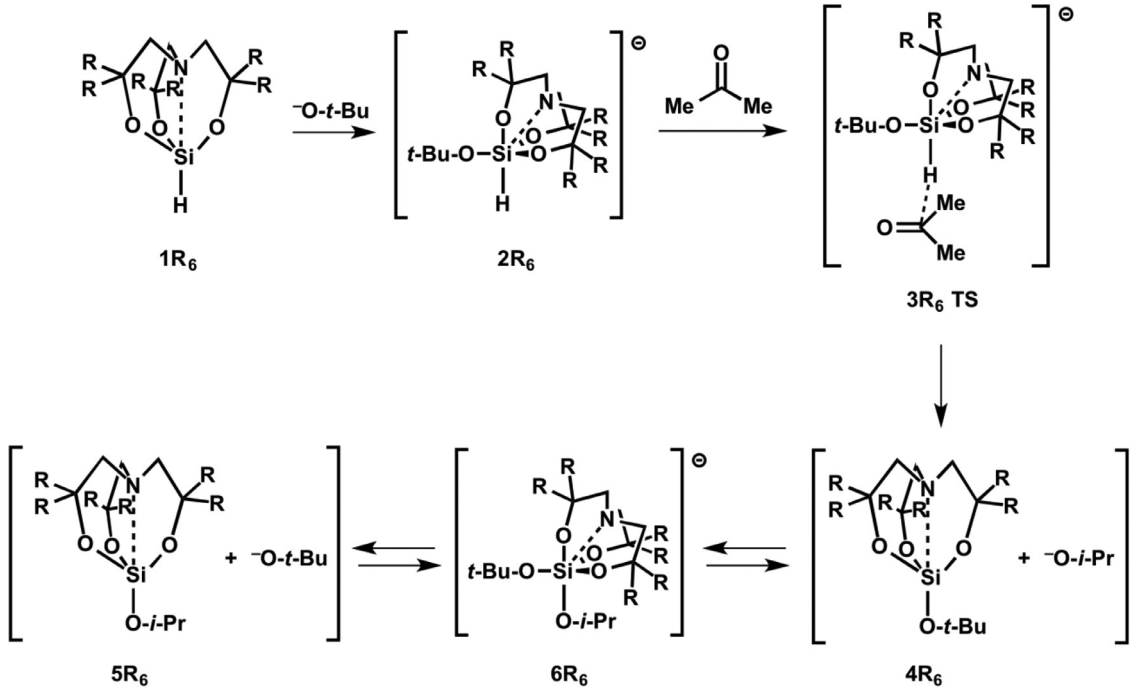

Scheme 2. Computationally derived mechanism of the reduction of acetone with hexasubstituted 1-hydridosilatranes.

Table 1
Optimized Si···N distances (pm) and QTAIM charge values (ωB97XD, e-) for parent silatrane **1H$_6$**, hexamethylsilatrane **1Me$_6$**, hexafluorosilatrane **1F$_6$**, 1-fluorosilatrane **1FH$_6$**, and 1-methylsilatrane **1MeH$_6$**.

Species	Si···N	*q*Si	*q*H	*q*O	*q*(alkoxy C)	*q*(amino C)	*q*N
1H$_6$	250.3	3.07	-0.69	-1.36	0.55	0.35	-1.11
1Me$_6$	240.8	3.07	-0.69	-1.37	0.55	0.34	-1.11
1F$_6$	234.9	3.07	-0.67	-1.36	1.69	0.34	-1.13
1FH$_6$	234.8	3.16		-1.35	0.55	0.34	-1.12
1MeH$_6$	264.2	3.09		-1.37	0.55	0.37	-1.12

ducing agents as efficacious as the parent while being more stable to solvolysis, soluble in a broader range of solvents, and differently chemoselective.

3.2. Mechanistic analysis

Initial optimizations involved examining the expected intermediates as computational minima. Numbering of the reaction components appears in Scheme 2; further labeling involves including an R$_6$ marker indicating which substituents are attached to the 3/7/10 alkoxy carbon positions. So **2Me$_6$** is intermediate component **2** in Scheme 2 with methyl groups at the alkoxy carbons. Transition states to be discussed later include the marker TS.

The structures of intermediates **2R$_6$, 4R$_6$, 5R$_6$**, and **6R$_6$** showed no unusual features, compounds **4R$_6$** and **6R$_6$** in particular exemplifying alkoxysilatranes in terms of bond distances and angles. Whether the R substituents were electron-neutral (H) or electron-withdrawing (F) had little impact on the cage bond distances; flu-

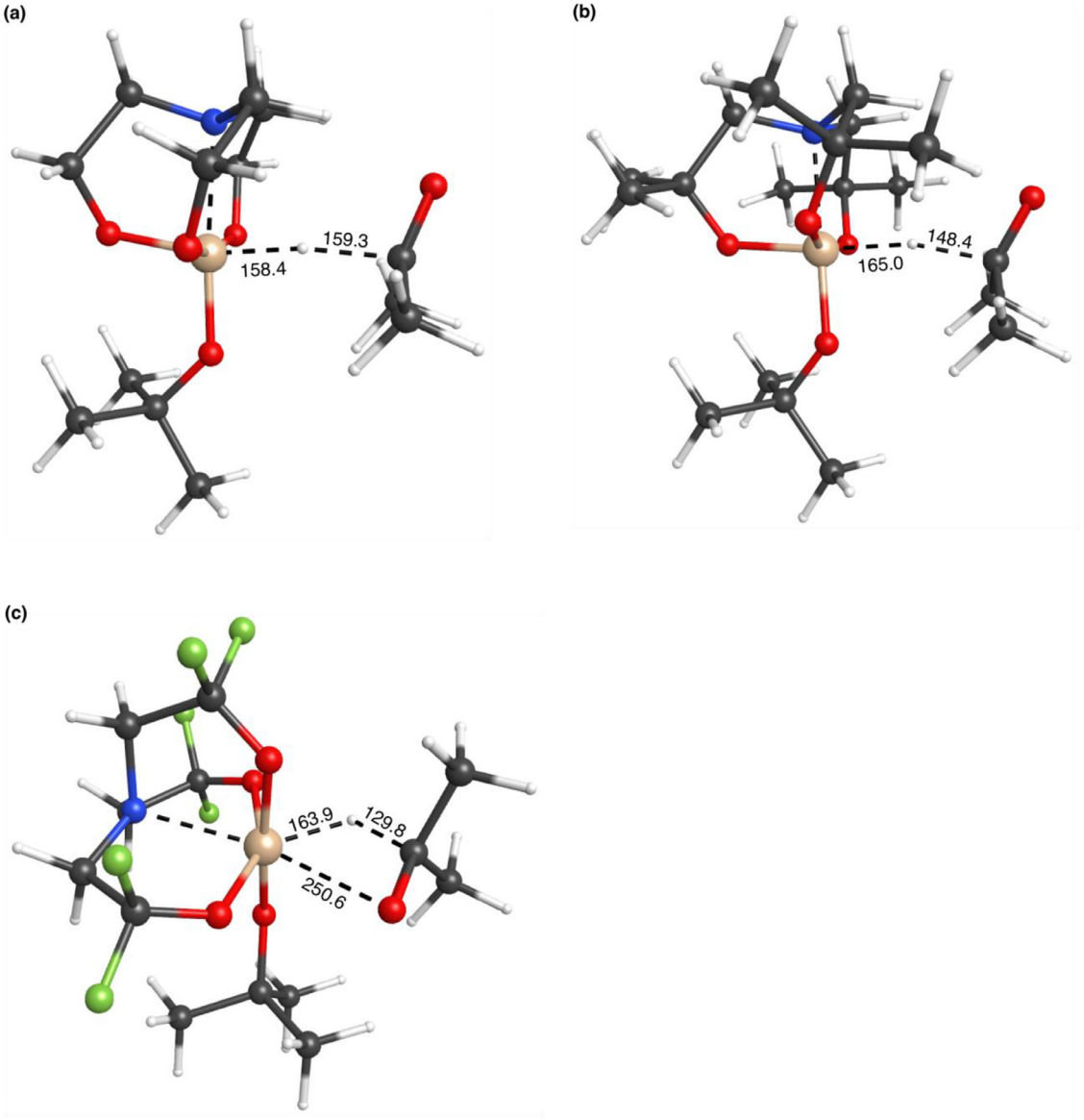

Fig. 3. Transition states 3R$_6$ TS with bond making/breaking distances (ωB97XD, pm). (a) 3H$_6$ TS; (b) 3Me$_6$ TS; (c) 3F$_6$ TS.

Table 2
Optimized Si···N distances (ωB97XD, pm) for mechanism components.

	$1R_6$	$2R_6$	$3R_6$ TS	$4R_6$	$5R_6$	$6R_6$
R = H	250.3	232.2	216.7	262.2	253.9	222.0
R = Me	240.8	221.8	214.4	244.7	240.6	212.2
R = F	234.9	210.4	226.1	247.9	239.4	211.4

orinated cages exhibited Si–O distances 2–3 pm longer and O–C distances 6–8 pm shorter than parent cages, but the C–C and C–N distances scarcely changed between the two (Supporting Information Table S4). This is consistent with the charge data described above, and makes it unlikely that electron donor/acceptor characteristics account for the reaction process differences described below. Intermediates **$2R_6$** and **$6R_6$,** with higher coordination numbers than **$4R_6$** and **$5R_6$**, exhibit considerably shorter Si···N distances (Table 2), reflecting the greater Lewis acidity of the Si as its coordination number increases.

The key steps of the reaction mechanism involve carbonyl compound coordination and subsequent hydride transfer, so we focused considerable attention on these. For all three silatranes, several types of relaxed scans of the potential energy surface (PES) for coordination made it clear that this step as shown in Scheme 1 is unlikely. Scans bringing the silicon and oxygen together demonstrated that coordination is a high-energy process for which no constraint-free stationary points could be located. As the carbonyl O atom approached the silicon, we saw considerable increases in the Si···N distances, to the point where the two were separated by the van der Waals distance of 340 pm. It seems likely that this arises because coordination of oxygen without loss of the Si···N interaction forces silicon to become seven-coordinate, an unlikely circumstance for a modestly sized main-group element. It appears that formation of the Si–carbonyl O interaction does not compensate for the resulting loss of the Si···N interaction, making carbonyl O coordination energetically unfeasible. Scheme 1 is thus flawed, explaining our alternative of Scheme 2 below.

Generally, the PES scans showed that species along the paths exhibited carbonyl C–Si distances that were shorter than the carbonyl O–Si distances. Moreover, scans bringing the carbonyl C and silicon-bound H into proximity showed lower path energies than did the Si–O scans above. Consequently we explored Scheme 2, where direct hydride transfer from silicon to the carbonyl carbon replaces the carbonyl coordination step in Scheme 1. Transition states **$3R_6$ TS** associated with this mechanism were located for R = H and Me, and appear as Fig. 3(a) and (b).

We note in passing that the isomer of **$2H_6$** shown in Fig. 3(a), with the H substituent *cis* to the cage N atom (H*cis*), is only 5 kJ mol^{-1} lower in Gibbs free energy than the H*trans* isomer where the silicon-bound H is *trans* to N (Supporting Information Table S3). To the degree that one can conceptualize six-coordinate silicon as being analogous to a six-coordinate transition metal, this is reasonably in keeping with the *trans* influence, which argues that a strong *trans* influencing substituent like H prefers to be *trans* to a weak influencing substituent like OR [42–44]. However, NR_3 is also a weak *trans* influencer, so the preference is likely small, a view supported here by the small energetic difference between isomers. One could envision that solvent or environmental effects could create an equilibrium between the isomers, and that possibly the H*trans* isomer would be the active reductant. We explored this by scanning the PESes associated with bringing the carbonyl oxy-

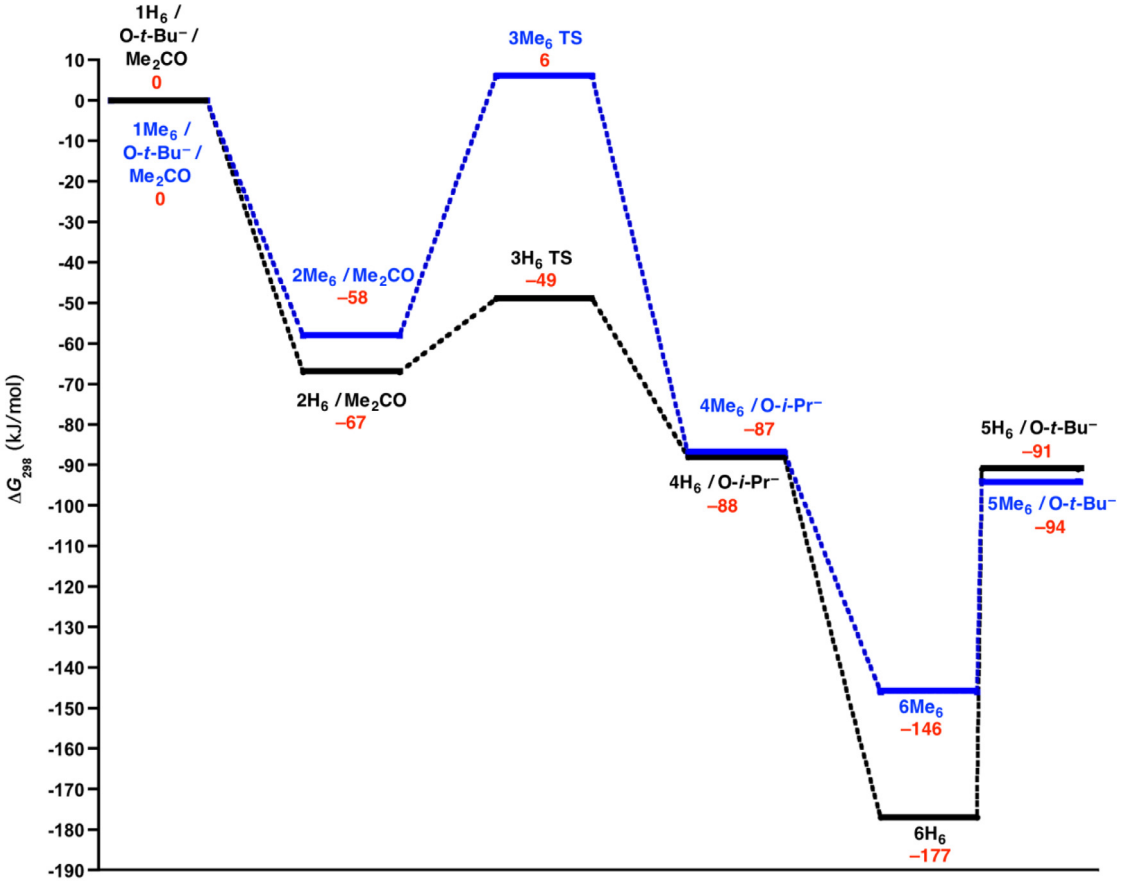

Fig. 4. Reaction coordinate diagram of Gibbs free energies (ωB97XD, numbers in red in kJ/mol) for the reduction of acetone by $1H_6$ (black lines) and $1Me_6$ (blue lines). (For interpretation of the references to color in this figure legend, the reader is referred to the web version of this article.)

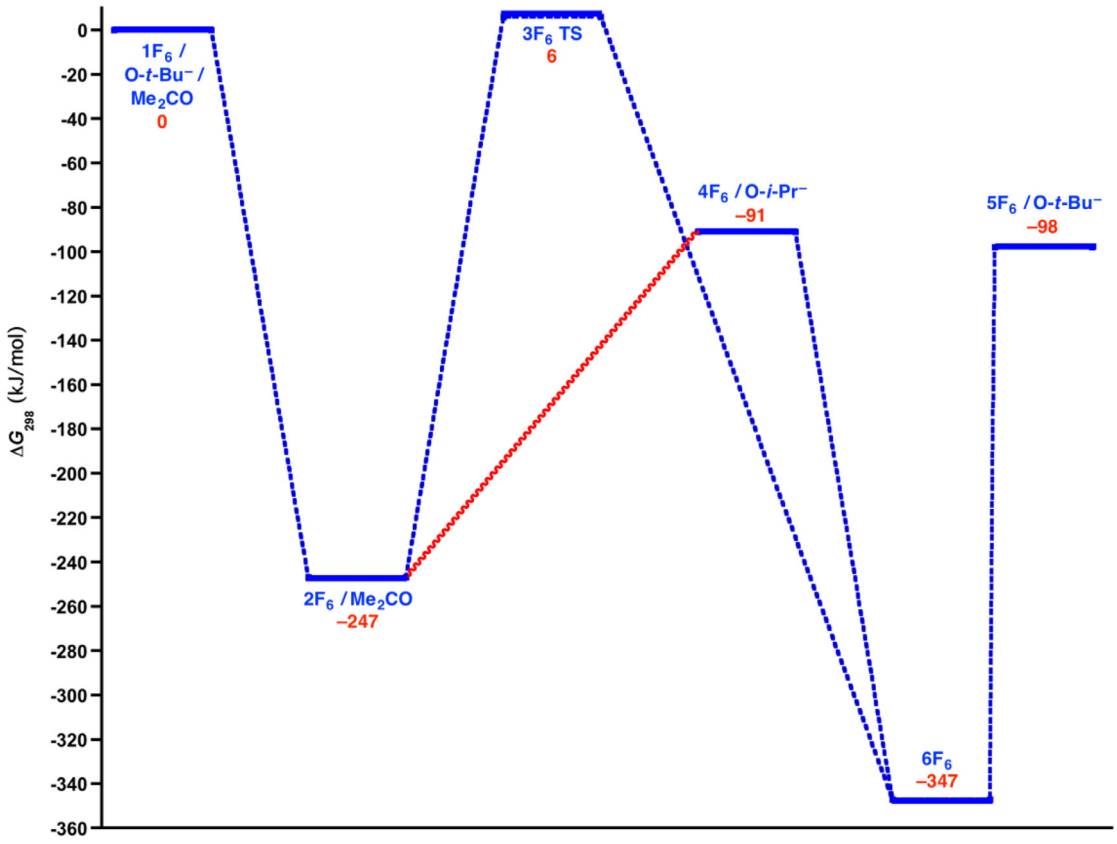

Fig. 5. Reaction coordinate diagram of Gibbs free energies (ωB97XD, numbers in red in kJ/mol) for the reduction of acetone by $1F_6$. The red squiggle is meant to show that transformation of $2F_6$ to $4F_6$/O-*i*-Pr$^-$ is highly endergonic, in contrast to the cases in Fig. 4. (For interpretation of the references to color in this figure legend, the reader is referred to the web version of this article.)

gen toward the silicon and/or the hydrogen to the carbonyl carbon for the H*trans* isomer. The former case resembled those described above wherein the energy rose and coordination did not occur; in the latter case, the energy rose and the hydrogen never transferred to the carbon. This proved true using a variety of scan probes. An example PES scan appears as Supporting Information Figure SF1. The H*trans* isomer of **2Me$_6$** lies 24 kJ mol^{-1} above the H*cis* isomer in Fig. 3(b), so the possibility of equilibrium is less likely. The greater preference for the H*cis* geometry here probably reflects a combination of the *trans* influence and steric repulsion; the O-*t*-Bu substituent in the H*trans* isomer interacts noticeably with cage methyl substituents, whereas interactions are far less significant in the H*cis* isomer (see Supporting Information Figure SF2). PES scans for this isomer also showed no coordination of carbonyl oxygen or ability to transfer hydrogen, although we did not test this as extensively as we did the parent.

3H$_6$ TS is a quite early transition state despite its similar Si···H and C···H distances owing to the larger size of Si. The Si···H distance is only 4% longer than that in **2H$_6$**, while the C···H distance is 45% longer than a typical C–H bond. Qualitatively, the electron-donating properties of the methyl substituents in **3Me$_6$ TS** should enhance hydride transfer and make this transition state lie earlier than for **3H$_6$ TS**; that this does not hold suggests that the steric repulsions between the methyl substituents and the incoming acetone overwhelm this and make **3Me$_6$ TS** lie later. The Si–acetone O distances in **3H$_6$ TS** and **3Me$_6$ TS** are 381.3 and 381.2 pm respectively, somewhat larger than the sum of the van der Waals radii of the atoms. The relevance of this will be discussed below.

Fig. 4 shows the reaction Gibbs free energy diagram associated with Scheme 2 and **1H$_6$/1Me$_6$**. One sees that each minimum lies energetically below the starting materials, with product dialkoxides **6H$_6$** and **6Me$_6$** occupying the lowest energy positions. Save for the transition states **3H$_6$ TS/ 3Me$_6$ TS**, the energetics for the two systems are similar. The difference between the two probably reflects the steric issues mentioned above. Reaching transition state **3Me$_6$ TS** from its starting materials is endergonic, but so little so that it seems likely that the reduction could be accomplished by raising the reaction temperature or by employing an appropriate solvent. Overall, it appears that **1Me$_6$** should be comparable to **1H$_6$** in reducing organic carbonyl groups. Given the higher barrier for hydride transfer, it is possible that **1Me$_6$** will prove more selective toward carbonyls with smaller substituents.

The plot shows that the energies of the ion/neutral pairs **4R$_6$/O-*i*-Pr$^-$** and **5R$_6$/O-*t*-Bu$^-$** lie significantly higher in energy than do the associated **6R$_6$** anions. Possibly inclusion of a polar solvent model or appropriate counterions would change this, so we cannot currently comment on the state of the equilibria in Scheme 2. We plan to explore this in more detail in the future.

Examination of the PES scans and optimized energies for species associated with reduction using hexafluoro **1F$_6$** indicted that the mechanisms in Schemes 1 or 2 were unlikely. As for the neutral/donor-substituted silatranes, oxygen coordination was a high-energy process, and hydride transfer as above proved implausible because formation of the **4F$_6$/**O-*i*-Pr$^-$ combination from the **2F$_6$/**Me$_2$CO pair proved endergonic by 156 kJ/mol (Fig. 5). This held despite the fact that formation of **6F$_6$** was exergonic from any stationary point. Indeed, **6F$_6$** lies so far below the **4F$_6$**/O-*i*-Pr$^-$ and **5F$_6$**/O-*t*-Bu$^-$ pairs that it is very unlikely either pair would form, so the equilibria in Scheme 2 would show exceedingly low equilibrium constants.

We believe this unexpected result arises because the Si–H bond in anionic **2F$_6$** is much stronger than the bond in **2H$_6$** or **2Me$_6$**, thus making transferring hydride from the anions to form neutral **4R$_6$** molecules less favorable. We tested this by determining the energetics of the reactions **2R$_6$** → **4R$_6$** + H$^-$ using the ωB97XD model. The R = H case was endergonic by 89 kJ/mol, while the R = F case was endergonic by 265 kJ/mol, supporting the hypothesis. Possibly the electronegative fluorines stabilize the negative charge in **2F$_6$** and make loss of hydride unfavorable. Unfortunately, QTAIM charge calculations did not confirm this unambiguously (Supporting Information Table S2).

As formation of **6F$_6$** is the goal of the reduction, it was clear that a mechanistic step forming this directly from **2F$_6$** was required rather than the two-step process used by **2H$_6$**/**2Me$_6$**. We examined the PES for possible one-step concerted processes, and located transition state stationary point **3F$_6$ TS** (Fig. 3(c)). **3F$_6$ TS** exhibits a much later transition state than **3H$_6$ TS**/ **3Me$_6$ TS** as gauged by the C–H distance, combined with a much smaller Si–O distance of 250.6 pm. It resembles the canonical transition state for transition metal σ-bond metathesis. [45] The barrier is only slightly higher than that for the Me analogue (Fig. 5). Thus the mechanism of reduction of acetone by **1F$_6$** is similar to that in Scheme 1, save that the hydrogen transfer is concerted rather than stepwise.

It should be noted that **3F$_6$ TS** arises from the H*trans* isomer of **2F$_6$**, which is 1 kJ mol^{-1} (ΔG_{298}) more stable than the H*cis* isomer, in contrast to **2H$_6$**/**2Me$_6$** (Supporting Information Table S3). This seems to run counter to the *trans* influence noted above, although obviously the preference is so small that it could represent model chemistry error. We are uncertain why the difference appears, although it may reflect the very small changes in the charges on the Si and N atoms between **2H$_6$** and **2F$_6$** (3.08/–1.11 *vs* 3.09/–1.16; see Supporting Information Table S2). Strong *trans* influencing substituents like H prefer to be *trans* to poorer donors; the larger positive charge on Si and larger negative charge on N indicate that N is a poorer donor in **2F$_6$**. Nonetheless, equilibrium between the two could exist in a solvent, so as above we performed PES scans using the H*cis* isomer. These behaved as did the higher energy isomers of the H/Me cases: no carbonyl oxygen coordination was observable, and hydrogen did not transfer to the carbonyl carbon.

We then examined the PESes to determine whether a concerted transition state was accessible for the H/Me cases. We located approximate structures for these analogous to **3F$_6$ TS**, but based on the H*cis* structures of **2H$_6$**/**2Me$_6$**. However, they proved >160 kJ/mol higher in energy than **3H$_6$ TS** and **3Me$_6$ TS**, making them mechanistically irrelevant. Consequently we did not optimize the structures further.

4. Conclusions

The charge distribution calculations indicated that the silatrane cage localized electronic effects of donor and acceptor substituents present at the alkoxy carbons, such that the hydridic nature of the silicon-bound hydride remained constant. This suggested that **1Me$_6$** and**1F$_6$** should reduce carbonyl groups as efficaciously as does the parent **1H$_6$**. The computational model confirmed this by providing energetics for the mechanism of reduction of the acetone carbonyl group by **1H$_6$**. The model determined the key detail that reduction does not require initial coordination of carbonyl oxygen to silicon.

Studies of reduction by **1H$_6$**/**1Me$_6$** showed similar mechanisms, with the latter exhibiting a slightly higher barrier that should be readily overcome under appropriate experimental conditions. This feature might confer the advantage of greater selectivity in reducing carbonyls. Moreover, the stability of 1-phenyl-3,3.7,7,10,10-hexamethylsilatrane toward hydrolysis suggests that reductions using **1Me$_6$** could be performed under aqueous or near-aqueous conditions, allowing for more economical and environmentally safe chemistry. (Some reductions using **1H$_6$** formed alcohols in modest yields in aqueous solution). Better still, the hydrolysis workup that converts **6H$_6$** to the alcohols and destroys the silatrane cage might only accomplish the first task for **6Me$_6$**, leaving intact something like 1-hydroxy-3,3.7,7,10,10-hexamethylsilatrane, which could be recycled via reduction to **1Me$_6$** using borohydride reductants or ideally H_2.

Reduction employing **1F$_6$** involves a lower barrier, and a slightly different, concerted hydride transfer transition state. This too could offer different selectivity, as well as the possibility of allowing reduction in fluorinated solvents or biphasic fluorosolvent/non-fluorosolvent mixtures.

The energetic favorability of the mechanisms for all three silatranes bodes well for future synthetic studies. Hexasubstituted silatranes might prove even more synthetically versatile than the parent. We hope experimentalists will prepare and examine the reactivities of hexasubstituted silatranes. In that regard, we have prepared 1-chloro- and 1-ethoxy-3,3.7,7,10,10-hexamethylsilatranes, and determined their crystal structures. Attempts to convert these to **1Me$_6$** are ongoing. We also plan further computational studies to address whether the mechanisms found above hold when bulkier ketones are reduced, why different chiral activators give different degrees of chirality in the product alcohols, and why the hydridosilatranes are selective toward aldehydes/ketones and do not reduce amides or esters.

Declaration of Competing Interest

The authors declare that they have no known competing financial interests or personal relationships that could have appeared to influence the work reported in this paper.

Acknowledgements

This research did not receive any specific grant from funding agencies in the public, commercial, or not-for-profit sectors. The NIU Computational Chemistry Laboratory was created using funds from the U. S. Department of Education and is supported in part by the taxpayers of the State of Illinois. The work used resources of the Center for Research Computing and Data at Northern Illinois University, specifically the Gaea computer cluster. We thank Sergey Uzunyan and Dave Ulrick of CRCD-NIU for their assistance and troubleshooting efforts.

Supplementary materials

Supplementary material associated with this article can be found, in the online version, at doi:10.1016/j.jorganchem.2021.122144.

References

[1] V.A. Pestunovich, S.V. Kirpichenko, M.G. Voronkov, Silatranes and their tricyclic analogs, in: Chem. Org. Silicon Compd., John Wiley & Sons, Ltd, 1998, pp. 1447–1537, doi:10.1002/0470857250.ch24.
[2] J.G. Verkade, Atranes: new examples with unexpected properties, Acc. Chem. Res. 26 (1993) 483–489, doi:10.1021/ar00033a005.
[3] J. Dillen, A quantum mechanical investigation of the nature of the dative bond in crystalline 1-chlorosilatrane, J. Phys. Chem. A. 108 (2004) 4971–4977, doi:10.1021/jp049155+.
[4] S.V. Belyakov, L.M. Ignatovich, E.J. Lukevics, Concerning the transannular bond in silatranes and germatranes: a quantum chemical study, J. Organomet. Chem. 577 (1999) 205–210, doi:10.1016/S0022-328X(98)01041-9.
[5] V.P. Feshin, E.V. Feshina, Nature of coordination bond in silatranes and its formation dynamics according to the ab initio calculations, Russ. J. Gen. Chem. 84 (2014) 70–74, doi:10.1134/S1070363214010101.
[6] T. Zöller, C. Dietz, L. Iovkova-Berends, O. Karsten, G. Bradtmöller, A.-K. Wiegand, Y. Wang, V. Jouikov, K. Jurkschat, Novel stannatranes of the type

$N(CH_2CMe_2O)_3SnX$ (X = OR, SR, OC(O)R, $SP(S)Ph_2$, halogen). Synthesis, molecular structures, and electrochemical properties, Inorg. Chem. 51 (2012) 1041–1056, doi:10.1021/ic202179e.
[7] S. Mun, S.H. Kim, J. Lee, H.-J. Kim, Y. Do, Y. Kim, Selective synthesis of monomeric or dimeric titanatranes via fine tuning in triethanolateamine ligand, Polyhedron 29 (2010) 379–383, doi:10.1016/j.poly.2009.06.017.
[8] G. Chung, O. Kwon, Y. Kwon, Molecular structure of 1-isothiocyanatosilatrane: Ab initio and DFT calculations, Inorg. Chem. 38 (1999) 197–200, doi:10.1021/ic980667a.
[9] M.G. Voronkov, E.I. Brodskaya, P. Reich, S.G. Shevchenko, V.P. Baryshok, Yu.L. Frolov, The influence of intermolecular interactions on the Si-H bond vibration in silatrane and its carbon substituents, J. Organomet. Chem. 164 (1979) 35–40, doi:10.1016/S0022-328X(00)83117-4.
[10] M.G. Voronkov, I.S. Emel'yanov, V.M. D'yakov, V.Yu. Vitkovskii, L.V. Kapranova, V.T. Baryshok, Atranes XLVIII, Chem. Heterocycl. Compd. 12 (1976) 1114–1116.
[11] C.L. Frye, R.L. Streu, Pentacoordinate silicon compounds. VI. A silatrane derived from tri-*tert*-butanolamine, Main Group Met. Chem. 16 (1993) 213–215.
[12] C.L. Frye, R.L. Streu, Pentacoordinate silicon compounds. VII. Solvolysis of some phenyl silatranes in acetic acid, Main Group Met. Chem. 16 (1993) 217–221.
[13] S. Sok, M.S. Gordon, A dash of protons: A theoretical study on the hydrolysis mechanism of 1-substituted silatranes and their protonated analogs, Comput. Theor. Chem. 987 (2012) 2–15, doi:10.1016/j.comptc.2011.08.011.
[14] M.G. Voronkov, V.P. Baryshok, S.N. Tandura, V.Y. Vitkovskii, V.M. D'yakov, V.A. Pestunovich, Atranes. L. C-Trifluoromethyl-substituted 1-organylsilatranes, J. Gen. Chem. USSR. 48 (1978) 2238–2245.
[15] D.N. Kursanov, Z.N. Parnes, G.I. Bassova, N.M. Loim, V.I. Zdanovich, Ionic hydrogenation of the ethylene bond and the double bond of the carbonyl group, Tetrahedron 23 (1967) 2235–2242, doi:10.1016/0040-4020(67)80059-0.
[16] M.B. Johansen, A.T. Lindhardt, Copper-catalyzed and additive free decarboxylative trifluoromethylation of aromatic and heteroaromatic iodides, Org Biomol Chem 18 (2020) 1417–1425, doi:10.1039/C9OB02635E.
[17] P.J. Kairisalo, A.H. Jarvinen, P.J. Hukka, New method for preparation of fluoxetine hydrochloride, FI 81083 (1990).
[18] M.T. Attar-Bashi, C. Eaborn, J. Vencl, R.D. Walton, Silatrane as a reducing agent, J. Organomet. Chem. 117 (1976) C87–C89.
[19] V. Skrypai, J.J.M. Hurley, M.J. Adler, Silatrane as a practical and selective reagent for the reduction of aryl aldehydes to benzylic alcohols, Eur. J. Org. Chem. (2016) 2207–2211.
[20] M.J. Adler, T.M. Gilbert, S.E. Varjosaari, V. Skyrypai, Preparation of alcohols from the reduction of ketones, aldehydes and iminiums with hydridosilatrane. US Patent 20170362151, 2017.
[21] S.E. Varjosaari, V. Skrypai, P. Suating, J.J.M. Hurley, T.M. Gilbert, M.J. Adler, 1-Hydrosilatrane: a locomotive for efficient ketone reductions, Eur. J. Org. Chem. (2017) 229–232.
[22] S.E. Varjosaari, V. Skrypai, S.M. Herlugson, T.M. Gilbert, M.J. Adler, Enantioselective metal-free reduction of ketones by a user-friendly silane with a reusable chiral additive, Tetrahedron Lett. 59 (2018) 2839–2843.
[23] S.E. Varjosaari, V. Skrypai, P. Suating, J.J.M. Hurley, A.M. De Lio, T.M. Gilbert, M.J. Adler, Simple metal-free direct reductive amination using hydrosilatrane to form secondary and tertiary amines, Adv. Synth. Catal. 359 (2017) 1872–1878, doi:10.1002/adsc.201700079.
[24] V. Skrypai, S.E. Varjosaari, F. Azam, T.M. Gilbert, M.J. Adler, Chiral bronsted acid-catalyzed metal-free asymmetric direct reductive amination using 1-hydrosilatrane, J. Org. Chem. 84 (2019) 5021–5026.
[25] R.R. James, S. Herlugson, S.E. Varjosaari, V. Skrypai, Z. Shakeel, T.M. Gilbert, M.J. Adler, One-pot reductive acetylation of aldehydes using 1-hydrosilatrane in acetic acid, SynOpen 03 (2019) 1–3, doi:10.1055/s-0037-1611697.
[26] G.L. Larson, J.L. Fry, Ionic and organometallic-catalyzed organosilane reductions, Org. React. 71 (2008) 1–737.
[27] R.J.P. Corriu, C. Guerin, K.A. Scheidt, R.B. Lettan II, G. Nikonov, L. Yunnikova, Triethoxysilane, e-EROS encyclopedia of reagents for organic synthesis (2014), 1-10.
[28] Y. Kobayashi, E. Takahisa, M. Nakano, K. Watatani, Reduction of carbonyl compounds by using polymethylhydrosiloxane: reactivity and selectivity, Tetrahedron 53 (1997) 1627–1634, doi:10.1016/S0040-4020(96)01092-7.
[29] J. Boyer, C. Breliere, R.J.P. Corriu, A. Kpoton, M. Poirier, G. Royo, Enhancement of Si–H bond reactivity in pentacoordinated structures, J. Organomet. Chem. 311 (1986) C39–C43, doi:10.1016/0022-328X(86)80263-7.
[30] R.J.P. Corriu, Hypervalent species of silicon: structure and reactivity, J. Organomet. Chem. 400 (1990) 81–106, doi:10.1016/0022-328X(90)83007-7.
[31] R. Schiffers, H.B. Kagan, Asymmetric catalytic reduction of ketones with hypervalent trialkoxysilanes, Synlett 1997 (2001) 1175–1178.
[32] M.J. Frisch, G.W. Trucks, H.B. Schlegel, G.E. Scuseria, M.A. Robb, J.R. Cheeseman, G. Scalmani, V. Barone, B. Mennucci, G.A. Petersson, et al., Gaussian 09 Rev E.01, Gaussian, Inc., Wallingford CT, 2009.
[33] J.-D. Chai, M. Head-Gordon, Long-range corrected hybrid density functionals with damped atom–atom dispersion corrections, Phys. Chem. Chem. Phys. 10 (2008) 6615–6620, doi:10.1039/B810189B.
[34] A.L. Gille, S.E. Hammer, J.M. Lafferty, K.R. Lawson, J.R. Gustafson, B.C. Dutmer, T.M. Gilbert, Computational studies of ene reactions between aminoborane $(F_3C)_2B{=}N(CH_3)_2$ and substituted propenes: additive effects on barriers and reaction energies, Dalton Trans. 48 (2019) 8161–8174.
[35] B.C. Dutmer, T.M. Gilbert, Computational studies of pericyclic reactions of aminoborane $(F_3C)_2B{=}N(CH_3)_2$: ene reactions vs. hydrogen transfers and regiochemical and conformational preferences, Organometallics 30 (2011) 778–791.
[36] J.R. Schmidt, W.F. Polik, WebMO version 19.0, WebMO LLC, Holland, MI, USA, 2019.
[37] Kaleidagraph for Macintosh version 4.5.4, Synergy Software, Reading, PA, USA, 2018.
[38] T.A. Keith, AIMAll version 19.10.12, TK Gristmill Software, Overland Park, KS, USA, 2019.
[39] R.F.W. Bader, Atoms in Molecules: A Quantum Theory, Oxford University Press, Oxford, 1990.
[40] R.F.W. Bader, A quantum theory of molecular structure and its applications, Chem. Rev. 91 (1991) 893–928, doi:10.1021/cr00005a013.
[41] R.F.W. Bader, Atoms in molecules, Acc. Chem. Res. 18 (1985) 9–15, doi:10.1021/ar00109a003.
[42] G.L. Miessler, P.J. Fischer, D.A. Tarr, Inorganic Chemistry, 5th ed., Pearson, Boston, 2014 Section 12.7.
[43] R.F. See, D. Kozina, Quantification of the *trans* influence in d^8 square planar and d^6 octahedral complexes: a database study, J. Coord. Chem. 66 (2013) 490–500.
[44] T.G. Appleton, H.C. Clark, L.E. Manzer, The trans influence: its measurement and significance, Coord. Chem. Rev. 10 (1973) 335–422.
[45] G.O. Spessard, G.L. Miessler, Organometallic Chemistry, Prentice-Hall, Upper Saddle River, NJ, 1997 Chapter 10-7.